09

Method for investigation of electromagnetic waves propagation characteristics of the optical and terahertz range in a metamaterials with a hyperbolic type of dispersion

© O.N. Kozina,[1] L.A. Melnikov[2]

[1]Saratov Branch, Kotel'nikov Institute of Radio Engineering and Electronics, Russian Academy of Sciences,
410019 Saratov, Russia
[2]Yuri Gagarin State Technical University of Saratov,
410054 Saratov, Russia
e-mail: kozinaolga@yandex.ru

Received January 13, 2025
Revised January 13, 2025
Accepted January 13, 2025.

The method for studying the propagation characteristics of optical and terahertz radiation in hyperbolic metamaterials at arbitrary angles of incidence, taking into account the anisotropy of the medium is present. The proposed numerical calculation method is effective for the most commonly studied types of hyperbolic metamaterials. This work aims to develop methods for studying composite structures to improve the component base for creating devices capable of generating and processing radiation in the optical and terahertz frequency ranges.

Keywords: metamaterial, nanoscale structure, hyperbolic medium, wire medium, multilayer structure

DOI: 10.61011/TP.2026.05.63530.358-25

Introduction

In recent decades, there's been a huge progress in the development of instrumentation base, including metamaterials — artificially created composite objects with predetermined properties [1]. Metamaterials are fabricated when it is necessary to get an object for specific purposes that does not exist in the natural environment. In this case, the so-called inverse problem is solved. A property that the object should posses is defined, and then a multicomponent metamaterial is artificially created. At the same time, the metamaterial has a certain geometric, generally, periodic structure. Depending on the geometry and types of its components, a metamaterial may have various properties. Metamaterials of various designs have unique electromagnetic properties that are unattainable using conventional, non-composite materials, which can be controlled by varying the parameters of the structure [1]. Research of various types of metamaterials, as well as methods of their fabrication, remain relevant for the scientific community both in terms of fundamental aspects and applied purposes [2]. Metamaterials open up new prospects in fabrication of devices for controlling the near electromagnetic field, including new types of electromagnetic sensors, lenses with subwavelength resolution, small-sized antennas, objects „invisible" in a certain range, phase plates, switching devices, high-quotient resonators, lenses, filters, reflectors, used for polarization control in VCSEL-lasers [1–4].

Various modifications are proposed, including metamaterials with a hyperbolic type of dispersion in the space of wave vectors — the so-called hyperbolic media (HM) [5–7]. HM is an anisotropic medium and got its name due to the open type of dispersion relations in the wave vectors space, which has the form of a hyperbola in cross section, unlike an ellipse for a conventional medium. HM were described in the middle of the XX century by F.I. Fedorov in his book „Optics of anisotropic media" [8], as well as in [9]. The most demonstrative natural object with hyperbolic properties is plasma in a strong electromagnetic field [8], as well as graphite and boron nitride under certain difficult conditions [10]. Along the asymptotes of hyperbolas, which are a cross section of isofrequencies in the space of wave vectors, numerous slow waves with large components of the wave vector are propagated. In other words, a high density of photonic states is observed inside HM, which leads to an increased interaction of radiation with the matter [11]. Metamaterials with such features are called hyperbolic metamaterials (HMM). HMM provide new capabilities for development of next-generation photonic devices, in particular, when creating an ideal radiation absorber, a terahertz radiation generator, and materials with thermal radiation exceeding the Planck limit. Therefore, the designing and study of metamaterials supporting the hyperbolic type of dispersion is a relevant task.

In our papers [7,12], we proposed a new concept of HMM — the so-called asymmetric hyperbolic metamaterial (AHMM). The AHMM is itself a periodic multilayer or „wire" structure in which the layers (rods) are located at an angle relative to the outer boundaries of the sample. The asymmetry manifests itself as a difference in the properties of the forward and reverse waves relative to the outer boundaries of AHMM, while the transverse component of the wave vector remains fixed. This structure is unique in terms of the variability of parameters, through which its properties are controlled [12]. Physically, the asymmetry is realized precisely by tilting the layers (rods) relative to the outer boundaries of the HM [7]. When a plane wave is incident on AHMM with minimal reflection from the sample's outer boundaries, a high density of photonic states is created inside the structure, which leads to a high rate of spontaneous emission. It is important that due to this asymmetry, photons with a high density of states excited in AHMM can have an ideal connection with photons in free space, which makes it possible to create conditions for the output of optical (or terahertz) radiation accumulated in the HM into the external space. Such an AHMM has significant amplification in the optical and terahertz (THz) frequency bands [7].

There are various ways to implement hyperbolic media [1,2,4,6,11], however, today two models of HMM are most often used: a multilayer periodic planar structure [13] and the so-called „wire medium“, consisting of a large number of metal rods of nanometer cross-section, periodically ordered in a dielectric matrix [14]. These types of HM structures allow them to be adapted for a wide range of wavelengths by selecting the appropriate parameters: the type of material, geometry, and the factor of filling the medium with material [7]. Studying the characteristics of electromagnetic waves in such structures is a difficult task and requires the development of new methods. Methods of studying the asymmetric hyperbolic structure require even more specific approaches.

This paper presents a method developed by the authors that makes it possible to study the propagation characteristics of optical and THz radiation in AHMM at an arbitrary angle of incidence on the structure, taking into account the anisotropy of the medium. The proposed numerical analysis is applicable for both layered and wire media.

1. AHMM

In general case, AHMM is a multilayer structure consisting of periodically alternating layers or rods of various materials located at a certain angle relative to the boundaries of the AHMM layer (Fig. 1). The asymmetry occurs due to the tilt of the optical axis (angle θ) relative to the outer boundaries of AHMM layer. The forward and reverse waves propagating in the structure acquire different properties due to this tilting while maintaining the components of the wave vector. As a result, conditions are created for the output of THz radiation generated in HM into the external space.

HMM, in general, are extremely anisotropic uniaxial media, the properties of which are described by the

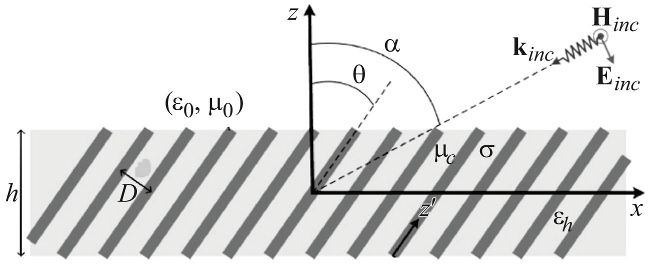

Figure 1. Schematic representation of AHMM. The oblique dark gray lines inside the AHMM symbolize graphene layers (or metal rods in the lateral projection). θ — angle between the optical axis and z axis (the angle of inclination of the optical axis), α — angle of incidence of radiation on the structure, h — total thickness of AHMM, D — period of AHMM.

dielectric constant tensor

$$\varepsilon = \begin{pmatrix} \varepsilon_{11} & \varepsilon_{12} & \varepsilon_{13} \\ \varepsilon_{21} & \varepsilon_{22} & \varepsilon_{23} \\ \varepsilon_{31} & \varepsilon_{23} & \varepsilon_{33} \end{pmatrix}_{xyz}$$

$$= \begin{pmatrix} \varepsilon_\perp + \Delta\varepsilon c_1^2 & \Delta\varepsilon c_1 c_2 & \Delta\varepsilon c_1 c_3 \\ \Delta\varepsilon c_1 c_2 & \varepsilon_\perp + \Delta\varepsilon c_2^2 & \Delta\varepsilon c_2 c_3 \\ \Delta\varepsilon c_1 c_3 & \Delta\varepsilon c_2 c_3 & \varepsilon_\perp + \Delta\varepsilon c_3^2 \end{pmatrix},$$

$$\Delta\varepsilon = \varepsilon_\parallel - \varepsilon_\perp.$$

Here the vector $c(c_1, c_2, c_3)$ is a unit vector parallel to the optical axis, $\varepsilon_\perp$ and $\varepsilon_\parallel$ are the values of the dielectric constant in the transverse and longitudinal directions of the considered structure, with $D = \varepsilon_\parallel E$ for $E \parallel c$ and $D = \varepsilon_\perp E$ for $E \perp c$.

In the case considered here, the components of sector c can be written as follows:

$$c_1 = \sin\theta \sin\varphi,$$

$$c_1 = \sin\theta \cos\varphi,$$

$$c_1 = \cos\theta.$$

Then, the tensor components ε are expressed as:

$$\varepsilon_{11} = \varepsilon_\perp + (\varepsilon_\parallel - \varepsilon_\perp)\sin^2\theta \sin^2\varphi,$$

$$\varepsilon_{12} = -(\varepsilon_\parallel - \varepsilon_\perp)\sin^2\theta \sin\varphi \cos\varphi,$$

$$\varepsilon_{13} = (\varepsilon_\parallel - \varepsilon_\perp)\sin\theta \cos\theta \sin\varphi,$$

$$\varepsilon_{21} = \varepsilon_{12},$$

$$\varepsilon_{22} = \varepsilon_\perp + (\varepsilon_\parallel - \varepsilon_\perp)\sin^2\theta \cos^2\varphi,$$

$$\varepsilon_{23} = -(\varepsilon_\parallel - \varepsilon_\perp)\sin\theta \cos\vartheta \cos\varphi,$$

$$\varepsilon_{31} = \varepsilon_{13},$$

$$\varepsilon_{32} = \varepsilon_{23},$$

$$\varepsilon_{33} = \varepsilon_\perp + (\varepsilon_\parallel - \varepsilon_\perp)\cos^2\theta.$$

It should be noted that for active media with gain or loss, $\varepsilon_\perp$ and $\varepsilon_\parallel$ have complex values.

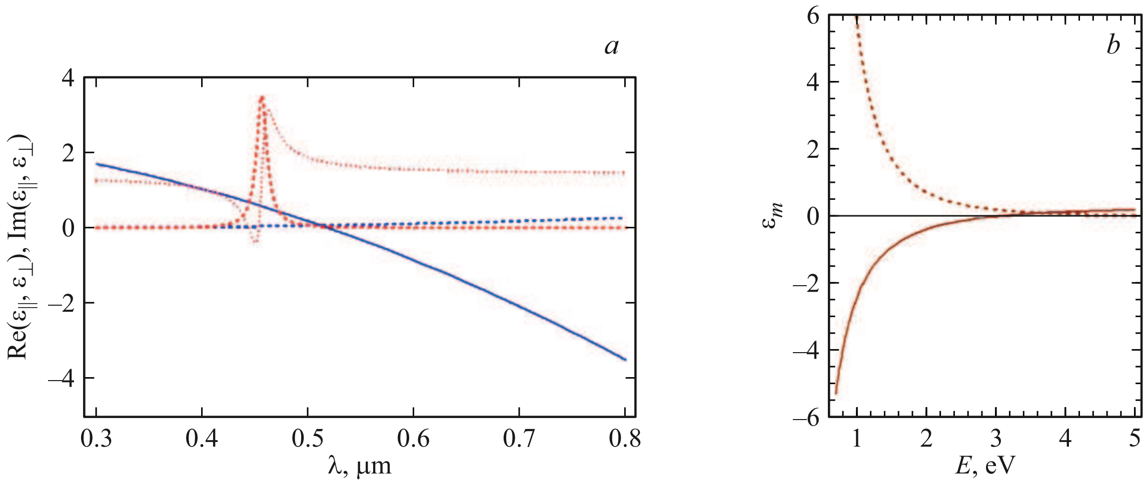

Figure 2. *a* — real (solid lines) and imaginary (dotted lines) parts of the longitudinal and transverse components of permittivity of the investigated AHMM depending on the wavelength in μm. $d_m = 30$ nm, $D = 70$ nm. *b* — real (solid line) and imaginary (dotted line) parts of the dynamic dielectric permittivity of gold, calculated based on Drude formula for the given sample as a function of energy in eV.

2. AHMM properties examination methods

Metamaterials, as a rule, have unit cell (period) values less than (or, as in this case, significantly less than) the wavelength of the radiation propagating in them. Due to these specific parameters, it becomes possible to describe their physical properties as a continuous (homogeneous) medium using the homogenization method. In this case, the composite structure is considered as an efficient medium with averaged parameters [7,15].

The diagonal components of an extremely anisotropic permittivity tensor are used to describe the optical parameters of hyperbolic media. In general, the effective relative permittivity tensor can be written as $\varepsilon = \{\{\varepsilon_\perp, 0, 0\}, \{0, \varepsilon_\perp, 0\}, \{0, 0, \varepsilon_\parallel\}\}$. The components of tensor acquire permittivity values in the longitudinal or transverse direction, depending on the geometry of the structure. In this case, the longitudinal component of the tensor $\varepsilon_\parallel = \varepsilon_h$ is dielectric permittivity of the base matrix material, the transverse component of the permittivity tensor $\varepsilon_\perp$ is the permittivity of the effective medium. For the hyperbolic medium the major values of the dielectric permittivity tensor $\varepsilon_\parallel$ and $\varepsilon_\perp$ have opposite signs [7,11].

Depending on the type of the considered AHMM, various methods of material homogenization can be used. In this paper, two main types of AHMM are considered: planar and rod-shaped.

In general, the planar structure consists of layers of material (metal or inverted graphene) periodically arranged in a dielectric (or semiconductor) matrix. If metal layers are used the effective parameters of the medium are calculated using the formulas [15]:

$$\varepsilon_\perp = \varepsilon_{xx} = \varepsilon_{yy} = f\varepsilon_m(\omega) + (1-f)\varepsilon_d,$$

$$\varepsilon_\parallel = \varepsilon_{zz} = \frac{\varepsilon_m(\omega)\varepsilon_d}{f\varepsilon_d + (1-f)\varepsilon_m(\omega)},$$

where $f = d_m/D$ — factor of the medium filling with metal, d_m — thickness of the metal layer, D —period of the structure, ε_d — dielectric permittivity of the dielectric, ε_m — dielectric permittivity of the metal.

Another version of AHMM structure is a so-called wire medium consisting of metal rods with a nanometer diameter, periodically alternating in a dielectric. Formulas [15,16] are used to determine the components of the dielectric permittivity tensor for AHMM of such geometry:

$$\varepsilon_\parallel = f\varepsilon_m(\omega) + (1+f)\varepsilon_d,$$

$$\varepsilon_\perp = \frac{(1+f)\varepsilon_m(\omega)\varepsilon_d + (1-f)\varepsilon_d^2}{(1-f)\varepsilon_m(\omega) + (1+f)\varepsilon_d},$$

where d_m — metal rod diameter. In both cases, the well-known Drude formula [17,18] is used to calculate the dielectric function of the metal.

As an illustration, some calculation results for both types of AHMM are given. AHMM consisting of metal rods periodically alternating in a dielectric is chosen as the wire structure. Gold was selected as a metal in this structure.

Fig. 2 shows the real and imaginary parts of the longitudinal and transverse components of the permittivity of a wire type AHMM based on gold rods, depending on the wavelength (Fig. 2, *a*), as well as the real and imaginary parts of the dynamic permittivity of gold, calculated from Drude formula for of the test sample (Fig. 2, *b*) [17,18].

The structure exhibit hyperbolic properties when $\mathrm{Re}(\varepsilon_\perp) < 0$. By the sign of the imaginary part of the effective permittivity of $\mathrm{Im}(\varepsilon_\perp)$, it is possible to determine in which frequency bands AHMM has a gain ($\mathrm{Im}(\varepsilon_\perp) < 0$) or absorption ($\mathrm{Im}(\varepsilon_\perp) > 0$). The graphs shown in Fig. 2 allow us to determine the range of wavelengths in which

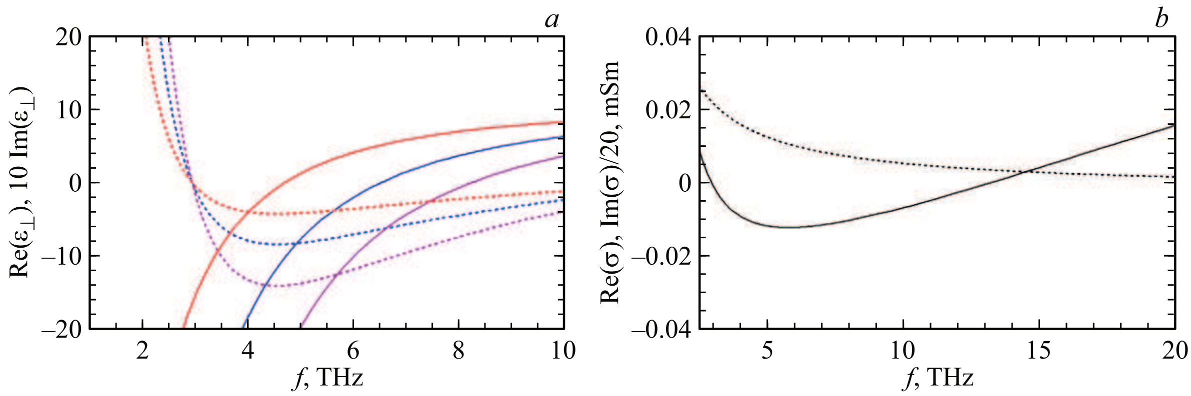

Figure 3. *a* — real (solid lines) and imaginary (dotted lines) parts of the effective permittivity versus frequency at different values of the structure period D (red lines — $D = 100$ nm, blue lines — $D = 50$ nm, magenta lines — $D = 30$ nm). *b* — real (solid line) and imaginary (dotted line) parts of graphene conductivity versus frequency at $E_F = 28$ MeV, $T = 300$ K, $t = 10^{-12}$ s.

both requirements are fulfilled simultaneously. This estimate makes it possible to model HMM for the required frequency ranges.

To demonstrate the results of the layered structure study, AHMM on inverted graphene was selected with its layers being periodically ordered in a semiconductor. The choice of different materials is justified by the significance of physical effects observed in them. Graphene layers are periodically ordered in a semiconductor (silicon carbide). In this case, the dielectric permittivity of the effective medium based on Maxwell-Garnett model is calculated using the formula

$$\varepsilon_\perp = \varepsilon_\parallel + \frac{i}{D\omega\varepsilon_0}[\sigma'(\omega, E_0) + i\sigma''(\omega, E_0)], \qquad (1)$$

where $\varepsilon_\parallel = \varepsilon_h$ — permittivity of the material in which graphene layers are located, ω — angular frequency, $\sigma(\omega, E_0)$ — surface conductivity of graphene, E_0 — transverse (relative to the plane of graphene sheets) component of the electric field strength vector, ε_0 — electrical constant, D — AHMM period. $\sigma(\omega, E_0) = (\sigma_{intra} + \sigma_{inter})$ — surface conductivity of inverted graphene, which depends on the frequency and component of the electric field vector transverse to the graphene plane. To calculate the conductivity of graphene layers, the Kubo formula was used (formula (2) from the work [18]). Variation of E_0 impacts the chemical potential μ_c. This approach provides a possibility to conduct a comprehensive analysis of the THz wave generation process in AHMM, taking into account the saturation effect of graphene amplification. In [12], an exact method for solving the dispersion equation for a periodic structure using Floquet-Bloch theorem and the homogenization method based on Maxwell-Garnett model is compared, and the results for the studied AHMM are shown to be completely consistent.

Fig. 3, *a* shows the curves of the real (solid lines) and imaginary (dotted lines) parts of the effective dielectric permittivity versus frequency at different values of the period of D, calculated using formula (1). As shown in the figure, the structure has hyperbolic and amplifying properties simultaneously at all three selected values of the structure period in a certain frequency range, which rises with the decreasing period. Figure 3, *b* shows a graph of the dependence of the real (solid lines) and imaginary (dotted lines) parts of the dynamic conductivity of graphene on frequency. It is known that condition $\mathrm{Re}[\sigma_{gr}(\omega)] < 0$ stands for the gain of energy, and condition $\mathrm{Re}[\sigma_{gr}(\omega)] > 0$ — corresponds to the energy losses. Therefore, using these calculations, it is possible to select the frequency range where amplification and generation of THz waves is predicted for a given value of Fermi energy.

By applying the homogenization formulas and calculating the values of the longitudinal and transverse components of the permittivity tensor, it is possible to determine the frequency ranges in which the considered structure has hyperbolic properties. It is known that hyperbolic properties are manifested when $\mathrm{Re}(\varepsilon_\perp) < 0$. Additionally, when studying the amplifying properties of the structure, the range in which it is possible to achieve significant radiation amplification is determined. For this, it is required to fulfill the condition $\mathrm{Im}(\varepsilon_\perp) < 0$. From the curves of $\mathrm{Re}(\varepsilon_\perp)$ and $\mathrm{Im}(\varepsilon_\perp)$ versus frequency these ranges are easily found.

3. Method of calculating the main characteristics of radiation propagation in AHMM

In HMM, abnormally high values of the density of electromagnetic states are observed along the asymptotes of hyperbolic frequencies in the space of wave vectors. As a result, numerous ordinary and unusual modes are excited, propagating in the forward and reverse directions inside the structure, which leads to a high rate of spontaneous emission. The study of these processes makes it possible to adapt such materials to the needs of technological goals, but new theoretical approaches are required. The study of

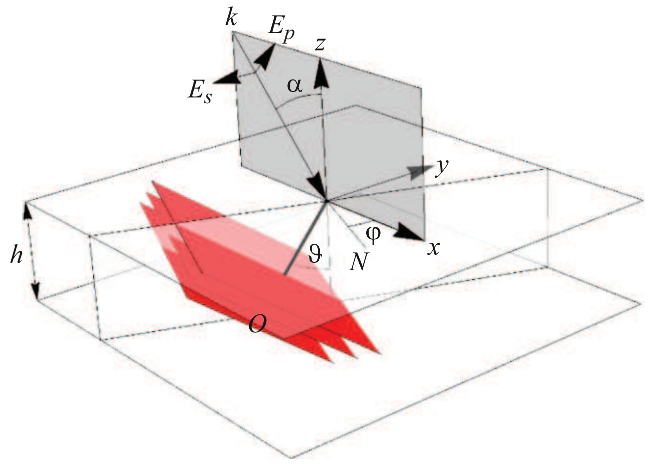

Figure 4. Schematic representation of a multilayer structure of AHMM with a demonstration of Euler angles. The red-colored surfaces symbolize layers (or tightly packed rods), O — optical axis, θ — angle between optical axis and axis z, N — node line, φ — angle between axis x and the line of nodes, α — the angle of radiation incidence on the structure, gray surface — plane of incidence, h — total thickness of AHMM.

physical processes occurring in AHMM is an even more difficult task due to the peculiarities of its geometry.

In this paper, to study the characteristics of electromagnetic waves propagating in AHMM, a method using Berreman matrix [19] is proposed and adapted, allowing to calculate the optical characteristics of forward and reverse waves in HM at an arbitrary angle of radiation incidence, given the anisotropy of the medium. The proposed numerical calculation method can be used for both layered and wire structures.

The use of formulas for AHMM homogenization makes it possible to study HM as an anisotropic medium with continuously changing parameters using Maxwell's equations in differential matrix form. In this case, the transformation between the four tangential components of the electric and magnetic fields at the input and output of the anisotropic optical system [19,20] is expressed by the formula with Berreman matrix Δ:

$$\frac{\partial}{\partial z}\Psi = \frac{i\omega}{c}\Delta\Psi.$$

The column vector Ψ generally contains all the tangential components of the electric and magnetic fields. In our consideration the column vector Ψ is written as:

$$\Psi = \begin{pmatrix} E_x \\ H_y \\ E_y \\ -H_x \end{pmatrix}.$$

The elements of Δ matrix are defined by expressions containing the components of the wave vector, components of the dielectric permittivity tensor of the effective medium, and Euler angles θ, φ, ψ [19,20]. Figure 4 schematically shows the AHMM in a coordinate system containing the given parameters. It should be underscored the red-colored layers can be either solid layers of some material, or layers consisting of multiple periodically arranged rods with a nanometer diameter. Overall thickness of AHMM — h. O — optical axis, N — nodes line, θ — angle between optical axis and z axis, φ — angle between x axis and nodes line, α — angle of radiation incidence on the structure, grey surface — incidence plane.

Having thus determined the parameters used, we write down the elements of Berreman matrix:

$$\Delta_{11} = -\frac{k_x}{K}\frac{\varepsilon_{zx}}{\varepsilon_{zz}}, \quad \Delta_{12} = 1 - \left(\frac{k_x}{K}\right)^2\frac{1}{\varepsilon_{zz}},$$

$$\Delta_{13} = -\frac{k_x}{K}\frac{\varepsilon_{zy}}{\varepsilon_{zz}}, \quad \Delta_{14} = -\left(\frac{k_x}{K}\right)\left(\frac{k_y}{K}\right)\frac{1}{\varepsilon_{zz}},$$

$$\Delta_{21} = \varepsilon_{xx} - \frac{\varepsilon_{zx}\varepsilon_{xz}}{\varepsilon_{zz}} - \left(\frac{k_y}{K}\right)^2, \quad \Delta_{22} = -\frac{k_x}{K}\frac{\varepsilon_{xz}}{\varepsilon_{zz}},$$

$$\Delta_{23} = \varepsilon_{xy} - \frac{\varepsilon_{zy}\varepsilon_{xz}}{\varepsilon_{zz}} + \left(\frac{k_x}{K}\right)\left(\frac{k_y}{K}\right), \quad \Delta_{24} = -\frac{k_y}{K}\frac{\varepsilon_{xz}}{\varepsilon_{zz}},$$

$$\Delta_{31} = -\frac{k_y}{K}\frac{\varepsilon_{zx}}{\varepsilon_{zz}}, \quad \Delta_{32} = -\left(\frac{k_x}{K}\right)\left(\frac{k_y}{K}\right)\frac{1}{\varepsilon_{zz}},$$

$$\Delta_{33} = -\frac{k_y}{K}\frac{\varepsilon_{zy}}{\varepsilon_{zz}}, \quad \Delta_{34} = 1 - \left(\frac{k_y}{K}\right)^2\frac{1}{\varepsilon_{zz}},$$

$$\Delta_{41} = \varepsilon_{yx} - \frac{\varepsilon_{yz}\varepsilon_{zy}}{\varepsilon_{zz}} + \left(\frac{k_x}{K}\right)\left(\frac{k_y}{K}\right), \quad \Delta_{42} = -\frac{k_x}{K}\frac{\varepsilon_{yz}}{\varepsilon_{zz}},$$

$$\Delta_{43} = \varepsilon_{yy} - \frac{\varepsilon_{yz}\varepsilon_{zy}}{\varepsilon_{zz}} - \left(\frac{k_x}{K}\right)^2, \quad \Delta_{44} = -\frac{k_y}{K}\frac{\varepsilon_{yz}}{\varepsilon_{zz}},$$

where $\mathbf{k} = (k_x, k_y, k_z)$ — wave vector, $K = \omega/c = 2\pi/\lambda$ — wave vector in vacuum. For active media with gain or loss, the components of the dielectric permittivity tensor $\varepsilon_\perp$ and $\varepsilon_\parallel$ have complex values. For a medium with a thickness of h, the electromagnetic fields of incident, reflected, and transmitted waves are related by the ratio

$$\mathbf{\Psi}_T = P(h)(\mathbf{\Psi}_I + \mathbf{\Psi}_R),$$

where $\mathbf{\Psi}_T$, $\mathbf{\Psi}_I$ and $\mathbf{\Psi}_R$ — column vectors of the transmitted, incident and reflected waves expressed as follows:

$$\mathbf{\Psi}_T = \begin{pmatrix} T_x \\ \frac{1}{\cos\alpha}T_x \\ T_y \\ \cos\alpha T_{yx} \end{pmatrix}, \ \mathbf{\Psi}_I = \begin{pmatrix} E_x \\ \frac{1}{\cos\alpha}E_x \\ E_y \\ \cos\alpha E_y \end{pmatrix}, \ \mathbf{\Psi}_R = \begin{pmatrix} R_x \\ -\frac{1}{\cos\alpha}R_x \\ R_y \\ -\cos\alpha R_y \end{pmatrix}.$$

Matrix $P(h)$ can be found by the formula

$$P(h) = e^{i\omega h\Delta/c} \equiv \sum_{k=1}^{4}\left(e^{i\omega h\lambda_k/c}\,\frac{\prod\limits_{i\neq k}(\Delta - \lambda_i I)}{\prod\limits_{i\neq k}(\lambda_k - \lambda_i)}\right),$$

where λ_{ik} — eigen values of the matrix Δ, I — unit matrix. This expression is an accurate representation of the function,

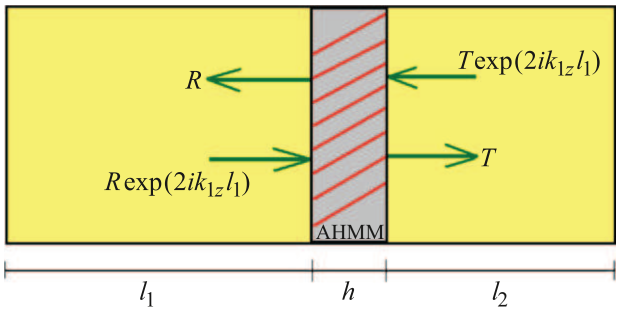

Figure 5. Schematic representation of a complex resonator, h — thickness of AHMM.

which eliminates the need to divide the environment into a system of sublayers. The eigen values of the matrix $\Delta - \lambda_{ik}$ — are found by the formulae

$$\lambda_{1,2} = \pm\sqrt{\varepsilon_\perp - \left(\frac{ck_x}{\omega}\right)^2},$$

$$\lambda_{3,4} = \left(-\frac{1}{\varepsilon_{33}}\right)\varepsilon\,\frac{ck_x}{\omega}\,\cos\theta\sin\varphi$$

$$\pm\left(-\frac{1}{\varepsilon_{33}}\right)\sqrt{\varepsilon_\perp(\varepsilon_\parallel\varepsilon_{33} - (\varepsilon_\parallel - \varepsilon\sin\theta\cos^2\varphi))\left(\frac{ck_x}{\omega}\right)^2},$$

where $\varepsilon_{33} = -\varepsilon_\perp\sin 2\theta + \varepsilon_\parallel\cos 2\theta$. In general case, the eigen values are the roots of a fourth degree polynomial $\det(\Delta - \lambda I) = 0$.

Using the above formulas, we can write expressions for calculating the transmission T and reflection R coefficients which are found as the ratio of the energy fluxes in the transmitted and reflected waves to the energy flux in the incident wave. They are written as

$$T = \frac{|T_x/\cos\alpha|^2 + |T_y|^2}{|E_x/\cos\alpha|^2 + |E_y|^2},$$

$$R = \frac{|R_x/\cos\alpha|^2 + |R_y|^2}{|E_x/\cos\alpha|^2 + |E_y|^2},$$

where T_x, T_y, R_x, R_y are calculated at given E_x, E_y by the formulae given in [19,20]. The results of calculation of the reflection and transmission spectra of AHMM are given in the work [7].

To tackle practical problems, the structure of HM and its surrounding regions of isotropic material is modeled. In this paper, we propose to consider a resonator with ideally reflecting walls, inside which a hypothetical AHMM with a thickness of h is located (Fig. 5).

The characteristics of radiation propagating in the resonator can be obtained as the eigen vectors of the product of the transmission matrices for the resonator medium (air or dielectric) $P_0(l_i)$ and Berreman matrix for the hyperbolic layer $P(h)$:

$$P_t = P_0(l_1 + l_2)P(h).$$

The eigen values of the resulting matrix P_t are found by the formula $\lambda_{ik} = \exp(i\cdot\varkappa_{ik}\cdot L)$, where $L = l_1 + l_2 + h$. By making this calculation, it is possible to obtain four eigen values for ordinary $(\varkappa_{1,2})$ and extraordinary $(\varkappa_{3,4})$ waves in the forward and reverse directions. The condition $\mathrm{Re}(\varkappa_{i,k}\cdot L) = 2\pi m$, $m = 0, \pm1, \pm2, \ldots)$ allows to determine the eigen waves in the resonator. The imaginary part of the eigen value $\mathrm{Im}(\varkappa_{i,k})$ characterizes possible enhancement in the structure. Therefore, the frequency of the resonator mode and intensity of this mode are solutions of the equations

$$\mathrm{Re}[\varkappa_i(k_z, E_0) = 0], \quad \mathrm{Im}[\varkappa_i(k_z, E_0) = 0].$$

The spectral dependences of the real and imaginary parts of the logarithms of the eigen values determine the ordinary and extraordinary eigen waves in the structure.

By calculating the eigen values and eigen vectors E_x, H_y, E_y, $-H_x$, we can calculate the time-averaged z component of the Poyting vector S_z, depending on the coordinate z due to gain (or loss), using the formula $S_z = E_xH_y^* - E_yH_x^*$. The sign before the calculated values z component of the Poyting vector makes it possible to identify forward and reverse waves. In addition, it is possible to determine which modes contribute to the „pure“ gain. These modes shall comply with $|\varkappa_i| > 1$, $S_z > 0$ or $|\varkappa_i| < 1$, $S_z < 0$.

This method allows studying the key characteristics of radiation propagating in the resonator, e.g., to analyze the reflection, transmission and absorption spectra, calculate the dependences of eigen values of the resonator transmission matrix characterizing the phase delay in one pass through the resonator, identify the frequency ranges where the studied structure has maximum gain, determine the frequency of wave generation, and calculate the dependencies of the Poyting vector components, which allows controlling the energy flows inside the structure, on the frequency in linear mode.

4. Examples of the method application

The given method allows for a theoretical study of the main characteristics of wave propagation both in the hyperbolic layer itself and in the resonator containing this layer.

Knowing the required frequency ranges (determined from the effective dielectric permettivity dependence on frequency), it is possible to calculate the eigen values of the transmission matrix and investigate various types of waves in the structure. Thus, two of the four eigen values (obtained within this theory) correspond to the forward and inverse ordinary waves, and two — to the forward and inverse extraordinary waves. By plotting the curves of the matrix eigen values versus frequency, it is possible to estimate the number of ordinary and extraordinary waves in the structure. It has been revealed that HM properties are enhanced precisely by extraordinary waves, the number of which increases many times with the appropriate selection

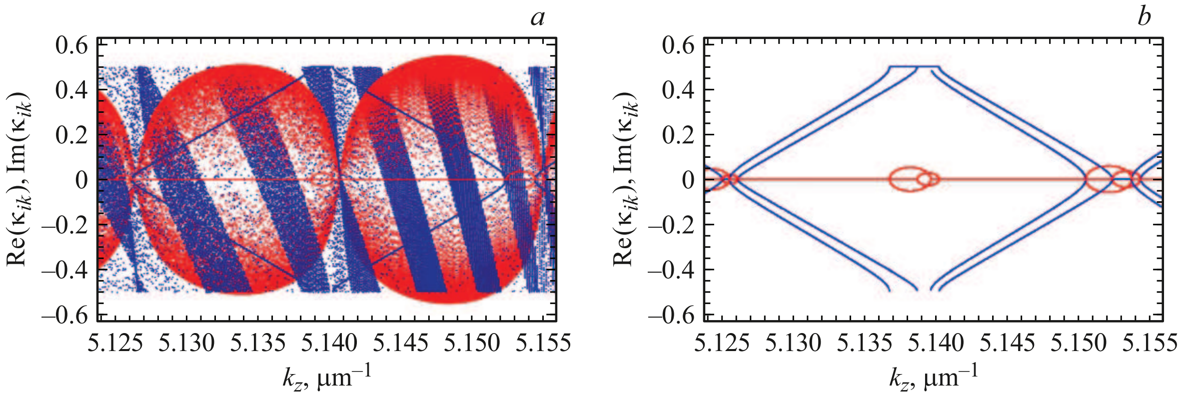

Figure 6. Real (blue curves) and imaginary (red curves) parts of the eigen values of ordinary $\varkappa_{1,2}$ and extraordinary $\varkappa_{3,4}$ waves versus z-component of the wave vector. $l_1 = 100\,\mu$m, $l_2 = 120\,\mu$m, $h = 1\,\mu$m, $d_m = 33$ nm, $D = 70$ nm; $k_x = \mathrm{tg}(\alpha)k_z$, $k_y = 0$, $\varepsilon_h = \varepsilon_\| = 3$. a — $\theta \approx \pi/3$, b — $\theta = 0$.

of the parameters of HMM and the resonator [21]. Thus, the AHMM highlighted here makes it possible to significantly increase the number of unusual modes by varying the optical axis inclination angle, which is also the angle of inclination of HM layers relative to its outer boundaries. The values of the layers' inclination angles are selected in each specific case so that the wave incident on AHMM undergoes minimal reflection. Next, the total length and period of AHMM, the diameter of the rods (or layers thickness) and parameters of the resonator in which it is located are selected for each specific type of material. By calculating these characteristics, it is possible to find optimal angle of radiation incidence on the structure for each case at which the predicted effects will be observed.

Demonstration shows the results of analyzing the waves of a complex resonator containing both types of AHMM: a wire and a layered structure. The layers' inclination angles, as well as other parameters, have different values for these specific examples. The types of HM listed here have different applications, and the results obtained for each type are not compared.

4.1. Resonator containing a wire medium AHMM structure

We have examined AHMMS of various configurations and consisting of components of various materials. The use of a particular type of AHMM to solve a specific problem was chosen by us as a result of a preliminary comprehensive assessment of its properties. For the generation of thermal radiation, a composite resonator containing a wire medium AHMM is the most promising. Having made appropriate selection the authors selected gold as a metal. The golden rods are periodically arranged in the glass in the form of a square grid. Figure 6 shows the dependences of the real and imaginary parts of each eigen value on z-component of the wave vector k_z. A dielectric with a permittivity $\varepsilon_h = \varepsilon_\| = 3$ was used as the material filling the resonator. Such a structure has the ability to accumulate thermal radiation in an amount exceeding the Planck limit.

To prove the effectiveness of using an asymmetric hyperbolic structure, the results for two different values of the orientation angle of the optical axis are demonstrated: $\theta \approx 0$ corresponds to a structure without asymmetry in which only two ordinary waves are observed (Fig. 6, b), and $\theta \approx \pi/3$ corresponds to an asymmetric hyperbolic structure where the number of modes, namely extraordinary waves, grows many times (Fig. 6, a). It was found that HM, in which the layers (rods) are located at an angle relative to the outer boundaries, allows not only to accumulate a high density of photonic states inside, but also to output the accumulated energy to the outer space.

The proposed theory also allows estimating the density of photonic states in a complex AHMM-containing resonator and finding the effect of a change in the orientation angle of the optical axis θ on the photonic states density in the structure. In previous studies, we have shown that with the synchronous selection of all parameters of AHMM and the resonator, it is possible to achieve an effective increase in the density of photonic states in the airy (isotropic) regions of the resonator [7,21].

Thus, based on the proposed theory, it is possible to study the features of radiation propagation in a resonator containing HM in order to assess the possibility of using such a structure as an element base in nanophotonics devices. In particular, an AHMM based on thin gold wires periodically arranged in a dielectric matrix can be used as a component base for optical devices, which opens up the possibility of creating new types of coherent and directional thermal radiation sources.

4.2. Resonator containing a multilayered structure AHMM

An AHMM consisting of layers of inverted graphene periodically arranged in a semiconductor matrix is considered as a multilayer plane-parallel structure. This type of

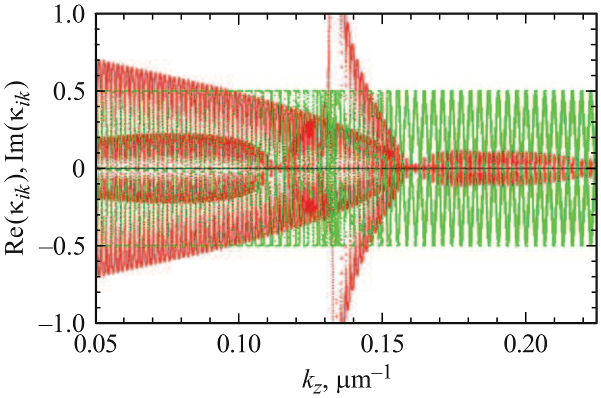

Figure 7. Eigen values $\varkappa_i$ of matrix P_t depending on k_z in the frequency range 2−12 THz ($0.051 < k_z < 0.225$). $\mathrm{Re}(\varkappa_{i,k})$ — green curves, $\mathrm{Im}(\varkappa_{i,k})$ — red curves; $l = 1320\,\mu$m, $h = 5\,\mu$m, $d = 30$ nm, Euler angles — $\varphi = \pi/2$, $\psi = 0$, $\theta = 55^\circ$. Radiation incidence angle on AHMM $\alpha = 15^\circ$; $E_F = 25$ meV, $T = 300$ K, $\tau = 10^{-12}$ s.

structure is promising for design of radiation sources in the terahertz frequency range. The calculations were performed taking into account the dynamic characteristics of graphene and silicon carbide [7]. The obtained dependences of the four eigen values for ordinary and extraordinary waves in the forward and reverse directions allow finding the THz wave gain, as well as the frequency of its generation. The main contribution to THz radiation gain comes from the extraodinary modes [21]. Developing this theory, we proposed a way to account for the saturation gain effect in graphene. However, this procedure is applicable only for this type of AHMM, that is why it is not included in the method described herein.

Thus, based on the proposed theory, it is possible to find the dependences of the eigen values of the resonator transmission matrix, which characterize the phase delay in one pass through the resonator, on the frequency in linear mode. The given spectral dependences of the real and imaginary parts of the logarithms of the eigen values make it possible to determine ordinary and extraordinary eigen waves in the resonator (Fig. 7). Either all four waves, or three, two, or only one of these waves can contribute to laser oscillations. The values of the imaginary part of the eigen value $\mathrm{Im}(\varkappa_i)$ characterize the gain in the structure. The losses were modeled by means of the complex dielectric permittivity of the resonator medium outside the AHMM. The introduction of losses inside the resonator avoids the need to impose boundary conditions. It was found that the gain in the studied structure significantly exceeds the loss level due to the presence of this type of AHMM allowing to multiply the number of extraordinary modes in the resonator. This example shows the possibility of generating THz radiation in a single-mode condition. The results obtained using the described method for a multilayer graphene-based structure can be used in modeling devices for generating radiation in the terahertz frequency band.

Conclusion

The method highlighted in this paper allows studying the propagation characteristics of optical and terahertz radiation in an AHMM at an arbitrary angle of incidence on the structure given the appropriate anisotropy of the medium. The proposed calculation method is effective for use in computational modeling of physical processes in the most frequently studied types of HMM when their parameters are replaced. Based on the proposed theory, it is possible to study the key characteristics of radiation propagating in AHMM, in particular, to analyze the reflection, transmission, and absorption spectra, find the dependences of the eigen values of resonator transmission matrix characterizing the phase delay in one pass through the resonator, estimate the density values of photonic states, and identify frequency bands in which the examined structure has maximum gain, determine the frequency of wave generation, as well as analyze the Poyting vector components, allowing to control the energy flows inside the structure, based frequency in a linear mode. Using the described method makes it possible to significantly simplify the assessment of the properties and capabilities of various types of HMM for their further use in the component databases to fabricate the devices that can generate and process radiation in the optical and terahertz frequency bands.

Funding

The study has been performed under the state assignment.

Conflict of interest

The authors declare that they have no conflict of interest.

References

[1] N.N. Schitov. Fotonika, **13** (8), 750 (2019) (in Russian). DOI: 10.22184/1993-7296.FRos.2019.13.8.750.759
[2] Yu.V. Gulyaev, A.N. Lagarkov, S.A. Nikitov. Vestnik RAN, **78** (5), 438 (2008) (in Russian).
[3] S.N. Petrov. *Fundamentalniye osnovy metamaterialov i ikh primeneniye v optike* (Ural University, Yekaterinburg, 2018) (in Russian).
[4] I.P. Sidorov. *Opticheskiye i akusticheskiye nanomaterialy: svoistva i primeneniya* (Nauka, SPb, 2017) (in Russian)
[5] I. Smolyaninov, V.N. Smolyaninova. Solid-State Electron., **136**, 102 (2017). DOI: 10.1016/j.sse.2017.06.022
[6] M.V. Davidovich. UFN, **189** (12), 1249 (2019) (in Russian). DOI: 10.3367/UFNr.2019.08.038643
[7] O.N. Kozina, L.A. Melnikov. Izvestiya Saratovskogo universiteta. Novaya seriya. Seriya Fizika, **19** (2), 122 (2019) (in Russian). DOI: 10.18500/1817-3020-2019-19-2-122-131
[8] F.I. Fedorov. *Optika anizotropnyh sred* (Academy of Sciences of the BSSR, Minsk, 1958)
[9] L. Felsen, N. Marcuvitz. *Radiation and scattering of waves* (A John Wiley & Sons, Inc, NY., 1973)

[10] J. Sun, J. Zhou, B. Li, F. Kang. Appl. Phys. Lett., **98** (10), 101901 (2011). DOI: 10.1063/1.3562033

[11] A. Poddubny, I. Iorsh, P. Belov, Yu. Kivshar. Nature Photon., **7**, 958 (2013).

[12] I.S. Nefedov, C.A. Valaginnopoulos, L.A. Melnikov. J. Opt., **15**, 114003 (2013). DOI: 10.1088/2040-8978/15/11/114003

[13] V. Iorsh, I.S. Mukhin, I.V. Shadrivov, P.A. Belov, Y.S. Kivshar. Phys. Rev. B, **87**, 075416 (2013). DOI: 10.1103/PhysRevB.87.075416

[14] C.R. Simovski, P.A. Belov, A.V. Atrashchenko, Y.S. Kivshar. Adv. Mater., **24**, 4229 (2012).

[15] S.M. Rytov. ZhETF, **29**, 5 (1955).

[16] C.L. Cortes, Z. Jakob. Phys. Rev. B, **88**, 045407 (2013).

[17] P.B. Johnson, R.W. Christy. Phys. Rev. B, **6**, 4370 (1972).

[18] A.A. Dubinov, V.Ya. Aleshkin, V. Mitin, T. Otsuji, V.J. Ryzhii. Phys. Condens. Matter, **23**, 145302 (2011). DOI: 10.1088/0953-8984/23/14/145302

[19] D.W. Berreman. J. Opt. Soc. Am., **62** (4), 1157 (1972).

[20] D.A. Yakovlev, V.G. Chigrinov. *Modeling and Optimization of the LCD Optical Performance* (Wiley, London, 2015)

[21] O.N. Kozina, L.A. Melnikov. Radiotekhnika i elektronika, **67** (10), 1058 (2022) (in Russian). DOI: 10.31857/S0033849422100060

Translated by T.Zorina